Shock-free Supersonic Transport

Problem presented by

Scott Rethorst

Vehicle Research Corporation

Problem statement

Vehicle Research Corporation has proposed a mechanism for eliminating the sonic boom generated by supersonic flight. It involves a nozzle-shaped wing underside, together with an underwing planar jet of engine compressor air. The Study Group was asked to provide a critical review of the proposed mechanism and a quantitative analysis of its likely performance.

Study Group contributors

P. Dellar (University of Cambridge)
J. Dewynne (University of Oxford)
C. Edwards (University of Oxford)
A. D. Fitt (University of Southampton)
P. D. Howell (University of Nottingham)
K. Kaouri (University of Oxford)
H. Ockendon (University of Oxford)
J. R. Ockendon (University of Oxford)
C. P. Please (University of Southampton)
D. Salazar-Gonzales (University of Oxford)

Report prepared by
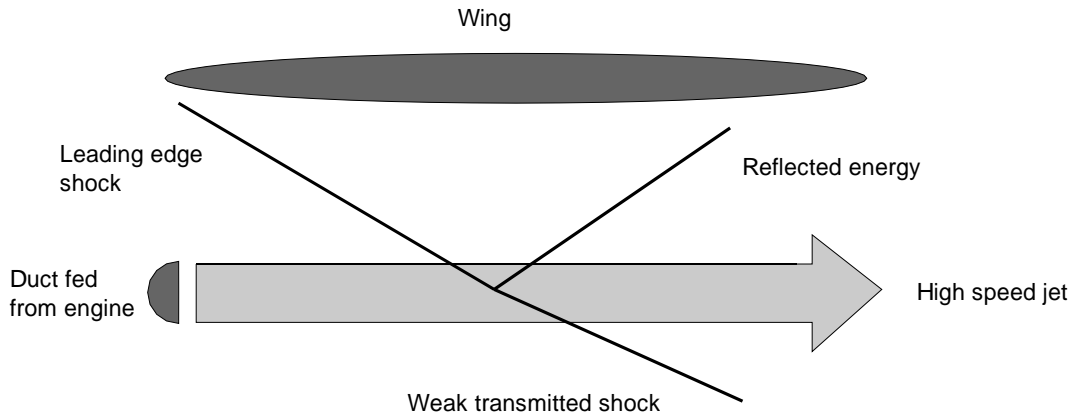
P. Dellar (with figure 6 supplied by P. D. Howell)

Figure 1: Sketch of a downward propagating shock reflecting off an underwing jet.

1   Introduction

Vehicle Research Corporation propose to reduce the environmental impact of supersonic transport aircraft using an underwing jet of high speed air to reflect the downward-propagating shock wave produced at the wing's leading edge. This jet reflection system is also intended to recover energy lost to dissipation in the shock. This configuration is sketched in Fig. 1, and described more fully in the problem description [1]. We did not consider the upward-propagating shock, which may be suppressed with a flat upper wing surface, as in the Busemann biplane, and in any case does not reach ground level.

We considered solutions of the steady, two-dimensional, compressible Euler equations for supersonic flow. These closely resemble the unsteady one-dimensional equations, the background supersonic flow determining the timelike direction, and admit the usual families of self-similar solutions: shocks, rarefactions waves or expansion fans, and contact discontinuities or vortex sheets [2, 3, 4]. We assumed the flow field could be described by regions of uniform flow separating appropriately chosen self-similar solutions.

We modelled the jet by two parallel vortex sheets enclosing a region of uniform higher speed flow. The compression waves generated at the wing's leading edge will typically steepen into shocks within a distance comparable with the wing's radius of curvature at the leading edge, so we assumed this happens before the compression wave reaches the underwing jet. The interaction between the jet and an incident shock may thus be broken down into two successive interactions between an incident shock and a vortex sheet of infinite extent. This is in contrast to the usually considered situation, where the collision of two shocks results in the formation of a semi-infinite vortex sheet and two reflected shocks. We subsequently discovered that our configuration, a shock reflecting off an infinite vortex sheet, is illustrated in Fig. 102(b,c) on page 423 of Landau & Lifshitz [3].
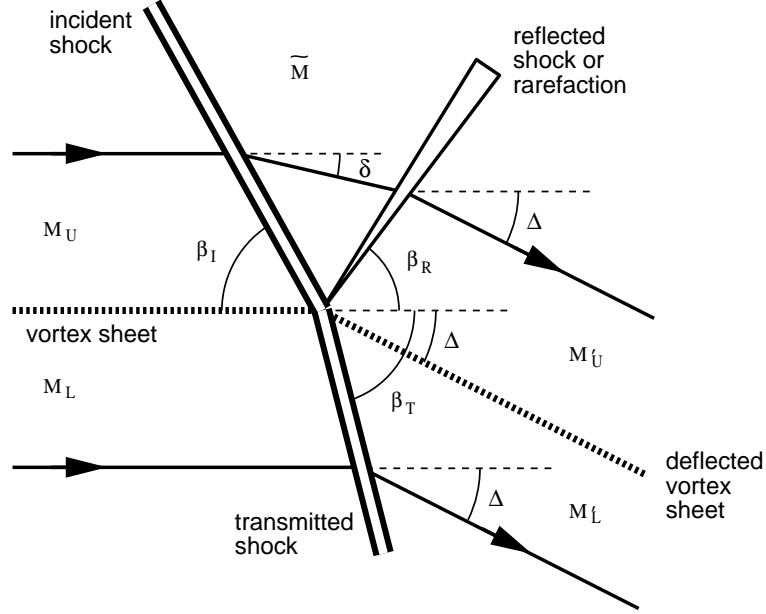
Figure 2: Sketch of a shock reflecting from a single vortex sheet

2 The upper vortex sheet

We considered an incident shock reflecting off a vortex sheet separating a slower flow on the incident side and a faster flow on the transmitted side. The geometry and notation is illustrated in Fig. 2. The angles β_I, β_R, β_T of the incident, reflected, and transmitted shocks respectively are measured from the direction of the incident vortex sheet, so as to lie between 0 and $\pi/2$ as illustrated.

From the Rankine-Hugoniot relations expressing conservation of mass, momentum, and energy in the direction normal to the incident shock, we obtain (eqs. 4.3, 4.7 & 4.10 of [4])

$$\frac{\tilde{p} - p}{p} \;\; = \;\; \frac{2\gamma}{\gamma + 1}(M_\mathrm{U}{}^2 \sin^2 \beta_\mathrm{I} - 1), \tag{1a}$$

$$\tilde{M}^2 \sin^2(\beta_\mathrm{I} - \delta) \;\; = \;\; \frac{1 + \dfrac{\gamma - 1}{2} M_\mathrm{U}{}^2 \sin^2 \beta_\mathrm{I}}{\gamma M_\mathrm{U}{}^2 \sin^2 \beta_\mathrm{I} - \dfrac{\gamma - 1}{2}}, \tag{1b}$$

$$\tan \delta \;\; = \;\; 2 \cot \beta_\mathrm{I} \frac{M_\mathrm{U}{}^2 \sin^2 \beta_\mathrm{I} - 1}{M_\mathrm{U}{}^2(\gamma + \cos 2\beta_\mathrm{I}) + 2}. \tag{1c}$$

M_U and M_L are the upstream Mach numbers above and below the vortex sheet, and $\tilde{M}$ is the Mach number in the sector between the incident and reflected shocks. Similarly, p is the upstream pressure, $\tilde{p}$ the pressure in the sector between the incident and reflected shocks, and p' is the downstream pressure. The ratio of specific heats is $\gamma = 1.4$ for a diatomic gas. The sign convention is such that $\delta \geq 0$, streamlines being deflected *towards* the shock line.

We obtain two equivalent sets of equations for the transmitted shock,

$$\frac{p' - p}{p} = \frac{2\gamma}{\gamma + 1}(M_{\mathrm{L}}{}^2 \sin^2 \beta_{\mathrm{T}} - 1), \tag{2a}$$

$$M_{\mathrm{L}}'{}^2 \sin^2(\beta_{\mathrm{T}} - \Delta) = \frac{1 + \dfrac{\gamma - 1}{2} M_{\mathrm{L}}{}^2 \sin^2 \beta_{\mathrm{T}}}{\gamma M_{\mathrm{L}}{}^2 \sin^2 \beta_{\mathrm{T}} - \dfrac{\gamma - 1}{2}}, \tag{2b}$$

$$\tan \Delta = 2 \cot \beta_{\mathrm{T}} \frac{M_{\mathrm{L}}{}^2 \sin^2 \beta_{\mathrm{T}} - 1}{M_{\mathrm{L}}{}^2(\gamma + \cos 2\beta_{\mathrm{T}}) + 2}, \tag{2c}$$

and the reflected shock,

$$\frac{p' - \tilde{p}}{\tilde{p}} = \frac{2\gamma}{\gamma + 1}(\tilde{M}^2 \sin^2(\beta_{\mathrm{R}} + \delta) - 1), \tag{3a}$$

$$M_{\mathrm{U}}'{}^2 \sin^2(\beta_{\mathrm{R}} + \delta - \Delta) = \frac{1 + \dfrac{\gamma - 1}{2} \tilde{M}^2 \sin^2(\beta_{\mathrm{R}} + \delta)}{\gamma \tilde{M}^2 \sin^2(\beta_{\mathrm{R}} + \delta) - \dfrac{\gamma - 1}{2}}, \tag{3b}$$

$$\tan(\delta - \Delta) = \frac{\tan \delta - \tan \Delta}{1 + \tan \delta \tan \Delta} = 2 \cot(\beta_{\mathrm{R}} + \delta) \frac{\tilde{M}^2 \sin^2(\beta_{\mathrm{R}} + \delta) - 1}{\tilde{M}^2(\gamma + \cos 2(\beta_{\mathrm{R}} + \delta)) + 2}. \tag{3c}$$

We have used the single variables p and p' for the upstream and downstream pressures, reflecting continuity of pressure across the vortex sheet. We may arbitrarily set the upstream pressure $p = 1$ since only ratios of pressures appear in these equations.

2.1 Solution procedure

We solved this set of nine equations for the nine unknowns Δ, δ, β_{I}, β_{R}, β_{T}, p', M_{U}', M_{L}' and $\tilde{M}$ in terms of the three input parameters M_{U}, M_{L} and $\tilde{p}/p$, the last of which denotes the incident shock strength. It proves more convenient to work in terms of the pressure ratios $\tilde{p}/p$ and p'/p instead of the shock angles β_{I}, β_{R} and β_{T}.

Each set of three equations determines conditions on the downstream side of a shock in terms of conditions on the upstream side. Since the supersonic flow provides a timelike direction, left to right as illustrated, information flows in the streamwise direction from left to right. However, two conditions must be imposed downstream of the transmitted and reflected shocks so that the upper and lower streamlines emerge parallel to each other and with equal pressures, necessary conditions for the existence of a vortex sheet. These conditions are implicit in the use of the same pressure p', and deflection angle Δ, in (2a-c) and (3a-c).

The first set of equations, (1a-c), may be solved directly for the incident shock angle β_{I}, and the quantities $\tilde{M}$ and δ in the sector between the incident and reflected shocks. Expressing β_{T} and $\beta_{\mathrm{R}} + \delta$ in terms of the pressures using (2a) and (3a), and substituting $\tan \delta$ and $\tan \Delta$ from (1c) and (2c) into (3c), we obtained a single algebraic equation relating $\tilde{p}/p$ and p'/p. Equations (2b) and (3b) may be used afterwards to determine the downstream Mach numbers M_{U}' and M_{L}'.
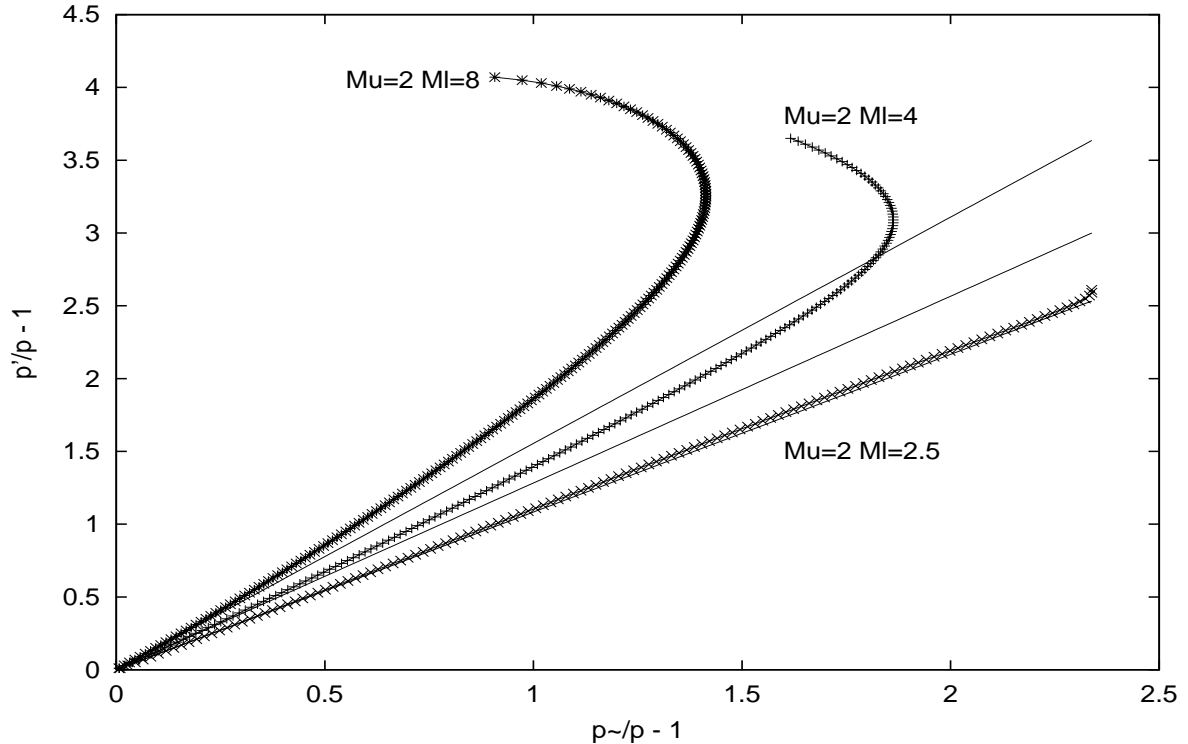
Figure 3: Transmitted shock strength $p'/p - 1$ versus incident shock strength $\tilde{p}/p - 1$. The weak shock theory is shown by straight lines, which is indistinguishable from the exact solution for $M_{\mathrm{U}} = 2$ and $M_{\mathrm{L}} = 2.5$.

2.2 Results

Numerical solutions of p'/p versus $\tilde{p}/p$ for various values of M_{U} and M_{L} are plotted in Fig. 3, and compared with the weak shock theory of §4. This solution with three shocks will only exist if the entropy condition for each shock is satisfied, in other words the pressure must *increase* downstream of each shock, and the normal velocity must *decrease* downstream of each shock. Based on the weak shock theory, these conditions will hold provided $M_{\mathrm{L}} > M_{\mathrm{U}} > \sqrt{2}$, at least for sufficiently weak incident shocks. We suspect the upper branches of numerical solutions in Fig. 3, between the maximum permissible incident shock strength and the point where the downstream pressure becomes imaginary, violate one or more of the these conditions, but we did not investigate which.

3   The lower vortex sheet

When the shock transmitted through the upper vortex sheet and the jet interior interacts with the vortex sheet on the lower jet boundary, it encounters a similar situation, except now with $M_{\mathrm{U}} > M_{\mathrm{L}}$. The reflected shock, which was assumed to exist in the above treatment, would thus be an unstable, or entropy violating, expansion shock, and has to be replaced by an entropy satisfying rarefaction wave, or expansion fan, of finite angular

extent. Thus the three equations (3a-c) are replaced by the two equations

$$\frac{p'}{\tilde{p}} = \left(\frac{1 + \dfrac{\gamma - 1}{2}\tilde{M}^2}{1 + \dfrac{\gamma - 1}{2}M_U'^2} \right)^{\frac{\gamma}{\gamma - 1}}, \tag{4a}$$

$$\Delta - \delta = \nu(M_U') - \nu(\tilde{M}), \tag{4b}$$

where $\nu(M)$ is the Prandtl-Meyer function (eq. 4.21b of [4])

$$\nu(M) = \sqrt{\frac{\gamma + 1}{\gamma - 1}} \tan^{-1} \sqrt{\frac{\gamma - 1}{\gamma + 1}(M^2 - 1)} - \tan^{-1}\sqrt{M^2 - 1}. \tag{5}$$

3.1 Solution procedure

The solution procedure is similar to before. Equations (1a-c) determine $\tilde{M}$, β_I and $\tan\delta$ from the input parameters M_U, M_L and $\tilde{p}/p$. Eliminating β_T using (2a), equation (2c) gives $\tan\Delta$ in terms of the unknown downstream pressure ratio p'/p. Equation (4a) determines M_U' from p'/p so that (4b), most conveniently rewritten in the form

$$\frac{\tan\delta - \tan\Delta}{1 + \tan\delta\tan\Delta} = \frac{\tan\nu(\tilde{M}) - \tan\nu(M_U')}{1 + \tan\nu(\tilde{M})\tan\nu(M_U')}, \tag{6}$$

becomes a single transcendental equation relating p'/p to $\tilde{p}/p$. This equation is transcendental, whereas the previous equation was algebraic, involving only polynomials and square roots, because of the ratio $(\gamma+1)/(\gamma-1)$ appearing in the function $\tan\nu(M)$.

3.2 Results

The results are shown in Fig. 4, and compared with the weak shock theory of §4. Again, the agreement with weak shock theory is adequate for the expected range of incident shock strengths.

4 Weak shock theory

We made further analytical progress by assuming that the incident shock is weak, in the sense that $\tilde{p} - p \ll p$. The incident shock angle β_I is then close to the Mach angle $\sin^{-1}(M_U^{-1})$, and equation (1c) simplifies to

$$\beta_I = \sin^{-1}\frac{1}{M_U} + \frac{1 + \gamma}{4}\frac{M_U^2}{M_U^2 - 1}\delta. \tag{7}$$

We have adopted the deflection angle δ as a small parameter, and discarded terms of $\mathcal{O}(\delta^2)$. Similarly, equations (1a,b) simplify to

$$\frac{\tilde{M}}{M_U} = 1 - \frac{\delta}{\sqrt{M_U^2 - 1}}\left(1 + \frac{\gamma - 1}{2}M_U^2\right), \tag{8a}$$

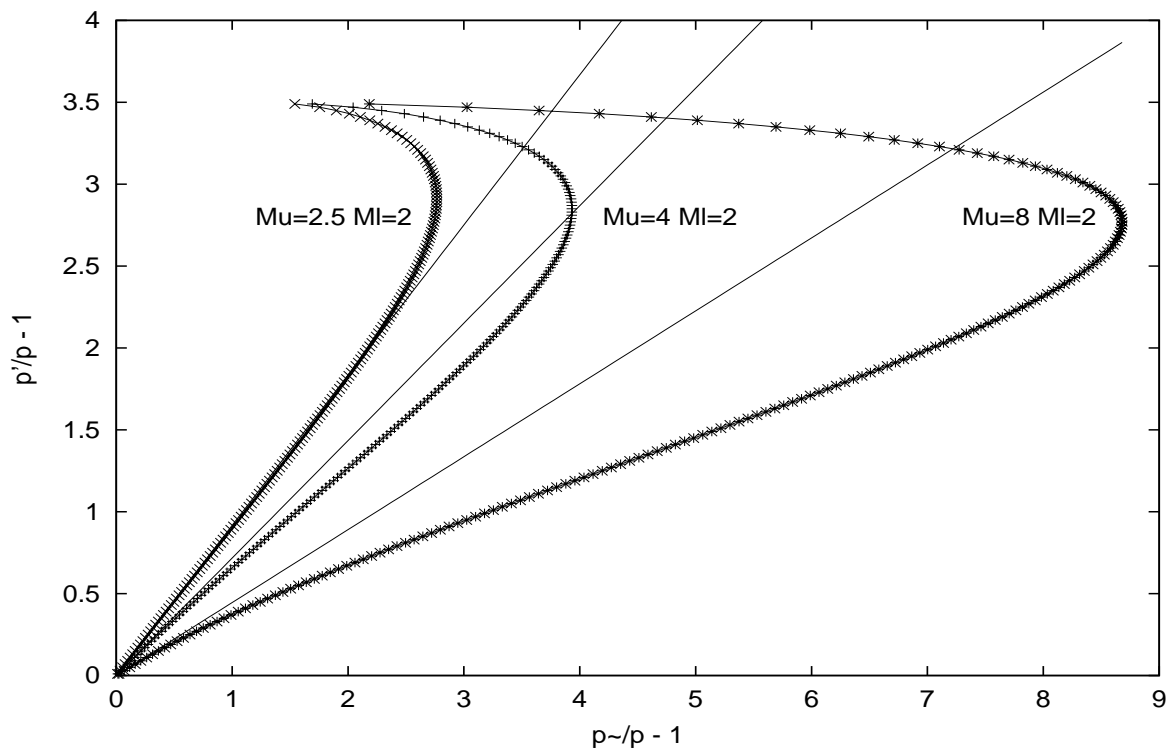$$\frac{\tilde{p}}{p} = 1 + \gamma\delta\frac{M_U^2}{\sqrt{M_U^2 - 1}}, \tag{8b}$$

Figure 4: Transmitted shock strength $p'/p - 1$ versus incident shock strength $\tilde{p}/p - 1$ for the lower vortex sheet, with a reflected rarefaction fan. The weak shock theory is shown by straight lines.

and the other two pressure equations (2a) and (3a) simplify to

$$\frac{p'}{p} = 1 + \gamma\Delta\frac{M_{\mathrm{L}}{}^2}{\sqrt{M_{\mathrm{L}}{}^2 - 1}}, \tag{9}$$

$$\frac{p'}{\tilde{p}} = 1 - \gamma(\Delta - \delta)\frac{M_{\mathrm{U}}{}^2}{\sqrt{M_{\mathrm{U}}{}^2 - 1}}. \tag{10}$$

The transmitted shock angle is

$$\beta_{\mathrm{T}} = \sin^{-1}\frac{1}{M_{\mathrm{L}}} + \frac{1+\gamma}{4}\frac{M_{\mathrm{L}}{}^2}{M_{\mathrm{L}}{}^2 - 1}\Delta, \tag{11}$$

and the reflected shock angle is

$$\beta_{\mathrm{R}} = \sin^{-1}\frac{1}{\tilde{M}} - \frac{1+\gamma}{4}\frac{M_{\mathrm{U}}{}^2}{M_{\mathrm{U}}{}^2 - 1}\Delta + \frac{1}{4}\frac{4 + M_{\mathrm{U}}{}^2(\gamma - 3)}{M_{\mathrm{U}}{}^2 - 1}\theta. \tag{12}$$

Eliminating $\tilde{p}$ and p' between (8b), (9) and (10), we obtain

$$\tilde{F}(\Delta - \delta) = F_{\mathrm{U}}\delta - F_{\mathrm{L}}\Delta, \tag{13}$$

where $\tilde{F} = F(\tilde{M})$ etc, or (since $\tilde{F} = F_{\mathrm{U}} + \mathcal{O}(\delta^2)$)

$$\Delta = \frac{2F_{\mathrm{U}}}{F_{\mathrm{U}} + F_{\mathrm{L}}}\delta. \tag{14}$$

The function $F(M) = M^2/\sqrt{M^2 - 1}$ is plotted in figure 5. It is monotonic increasing for $M > \sqrt{2}$. We can also relate the pressure jumps via

$$\frac{p' - p}{\tilde{p} - p} = \frac{2F_{\mathrm{L}}}{F_{\mathrm{L}} + F_{\mathrm{U}}}, \tag{15}$$

so the transmitted shock is stronger than the incident shock if $F_{\mathrm{L}} > F_{\mathrm{U}}$, and weaker otherwise.

If $\Delta < \delta$ we have three shocks, as in §2, and if $\Delta > \delta$ we have an expansion fan as in §3. In the proposed supersonic flight regime we have $M_{\mathrm{L}} > M_{\mathrm{U}} > \sqrt{2}$, giving a reflected shock from the upper vortex sheet and a reflected rarefaction wave from the lower vortex sheet.

4.1   A weak reflected rarefaction wave

For a weak incident shock, the linearised expression for the pressure ratio $p'/\tilde{p}$ across a weak reflected rarefaction wave obtained from (4a-b) coincides with that obtained from
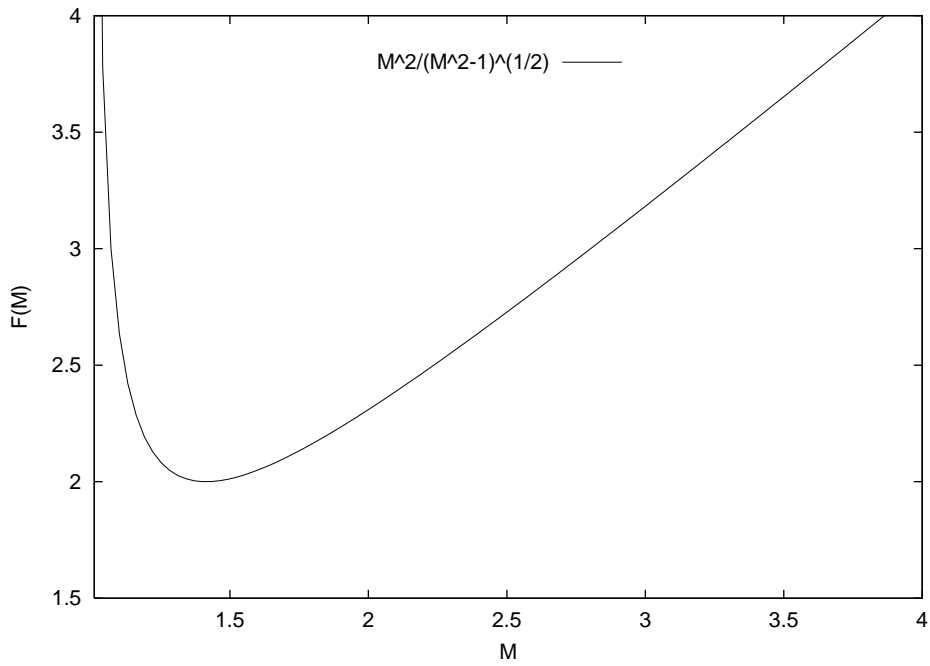
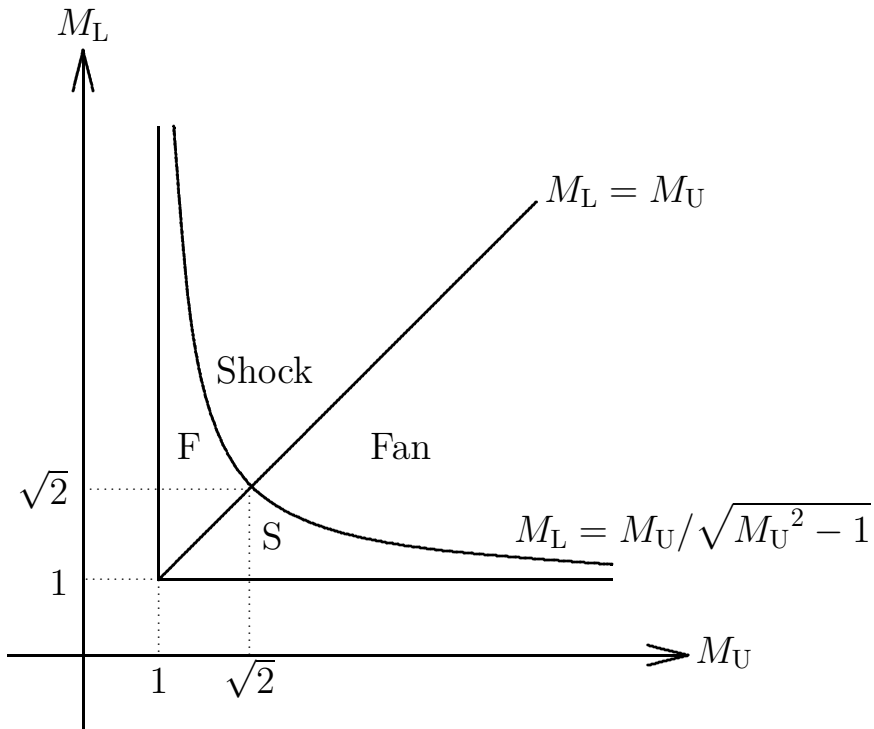Figure 5: Graph of the function $F(M) = M^2/\sqrt{M^2 - 1}$ from §4.

Figure 6: Regime diagram showing when a weak incident shock produces a reflected shock (S) or expansion fan (F), for varying Mach numbers M_U and M_L.

(3a-c) for a weak reflected shock,

$$
\begin{aligned}
\frac{p'}{\tilde{p}} &= 1 + \frac{\gamma M_{\mathrm{U}}}{1 + \dfrac{\gamma - 1}{2} M_{\mathrm{U}}{}^2}(\tilde{M} - M'_{\mathrm{U}}), \\[2em]
&= 1 + \frac{\gamma M_{\mathrm{U}}}{1 + \dfrac{\gamma - 1}{2} M_{\mathrm{U}}{}^2}(\Delta - \delta)\Big/\frac{d\nu}{dM}\Big|_{M = M_{\mathrm{U}}}, \\[2em]
&= 1 - \frac{\gamma M_{\mathrm{U}}}{\sqrt{1 - M_{\mathrm{U}}{}^2}}(\Delta - \delta). \quad\quad (16)
\end{aligned}
$$

Thus the above theory applies equally to weak reflected shocks and weak reflected rarefaction waves.

5   Shock/jet interaction

As explained in the introduction, we treated the jet as a uniform stream separated from the slower background flow by two vortex sheets. Applying the above calculation twice, to the upper and lower vortex sheets, we obtain the attenuation factor for weak shocks passing through the jet,

$$
\frac{p_{\mathrm{I}} - p}{p_{\mathrm{T}} - p} = \frac{4 F_{\mathrm{L}} F_{\mathrm{U}}}{(F_{\mathrm{L}} + F_{\mathrm{U}})^2}, \quad\quad (17)
$$

which is plotted in figure 7 for a Mach 2 background flow. Figures 3 and 4 suggest that the weak shock approximation is adequate for plausible incident shock strengths, *i.e.* $p_{\mathrm{I}} < 2p$.

6   Conclusion

If the jet is treated as a region of uniform flow, bounded by two parallel vortex sheets, the jet reflects very little of the incident shock at plausible jet speeds. Most of the attenuation that takes place when the shock passes across the upper vortex sheet into the jet is undone by the passage through the the lower vortex sheet back into ambient air. Vehicle Research Corporation proposed [5] that overpressure in the jet, *i.e.* a jump in pressure across what we took to be a vortex sheet with continuous pressure, would increase the proportion of energy reflected. However, a consistent treatment would require a relation similar to equations (1a-c) for the pressure jump, which we could not derive.

It should be possible to extend our treatment to more complex jet profiles by modelling the jet as a finite collection of uniform streams separated by vortex sheets, and applying the above analysis to each internal boundary. So far we have ignored any subsequent downward reflections of upward-propagating reflected fans or shocks, for instance the reflection of the upward propagating rarefaction fan by the upper vortex sheet, but this may have to be revised.

The two regimes giving reflected shocks or rarefaction waves reverse for Mach numbers below $\sqrt{2}$, where $f(M)$ is monotonic *decreasing*, as illustrated in figures 5 and 6. For
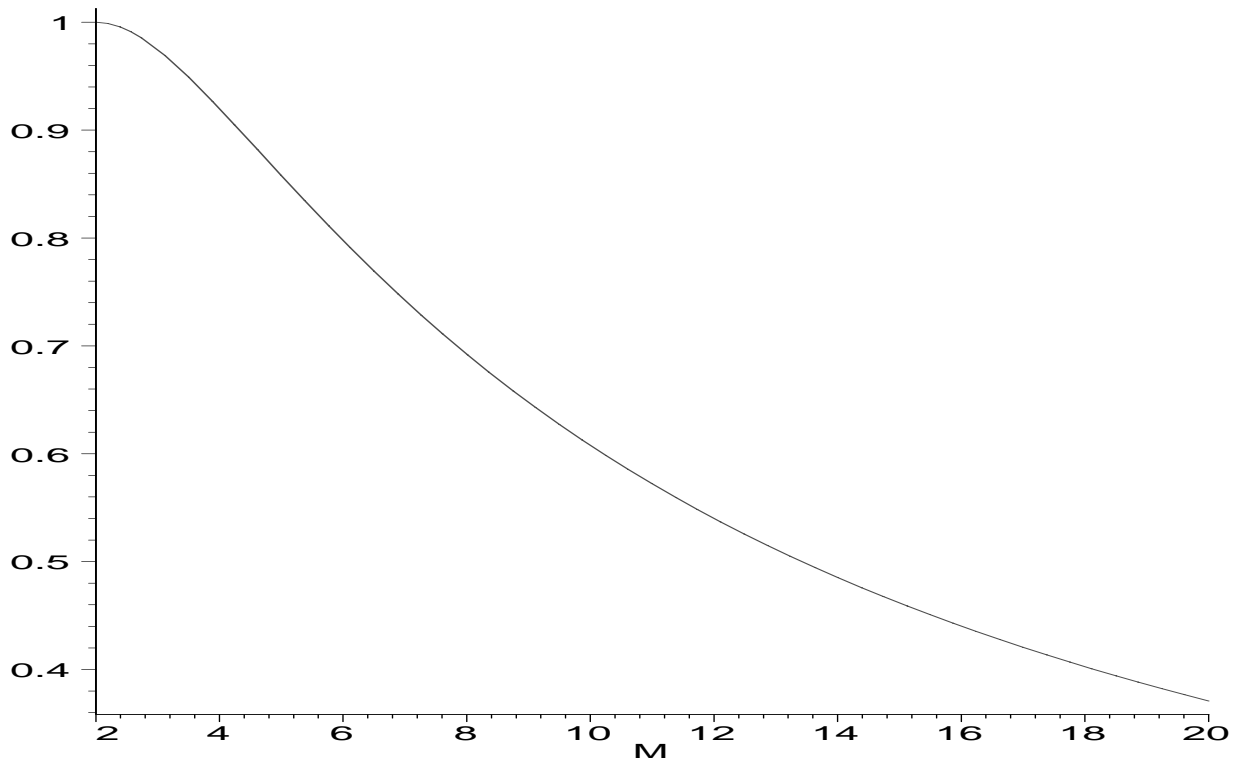
Figure 7: Weak shock attenuation factor for a Mach 2 aeroplane as a function of the jet Mach number M. Note that the proposed jet speed $M = 4$ only gives an 8% attenuation.

$M < \sqrt{2}$, we predict a reflected rarefaction wave from the upper vortex sheet, and a reflected shock from the lower vortex sheet. The behaviour at slightly supersonic speeds during acceleration, $M < \sqrt{2}$, will likely differ from the intended behaviour at cruising speeds, $M > \sqrt{2}$.

References

[1] Shock free supersonic flight. Vehicle Research Corporation. Problem description for ESGI 2001, Keele, April 9th-12th 2001.

[2] R. Courant and K.O. Friedrichs. *Supersonic Flow and Shock Waves*. Springer-Verlag, New York, 1976. (First published Wiley-Interscience 1948).

[3] L. D. Landau and E. M. Lifshitz. *Fluid Mechanics*. Pergamon, Oxford, 2nd edition, 1987.

[4] H. W. Liepmann and A. Roshko. *Elements of Gasdynamics*. Wiley, New York, 1957.

[5] S. Rethorst and E. James. Enhanced compression wave reflection from a real fluid shear layer employing acoustic excitation. Technical Report VRC Working Paper No. 315, Vehicle Research Corporation, 61 South Lake Avenue, Pasadena, CA 91101, USA, 1985.